NAVAL POSTGRADUATE SCHOOL
Monterey, California

AD-A275 983

‖‖‖‖‖‖‖‖‖‖‖‖‖‖‖‖‖‖

DTIC
ELECTE
FEB 24 1994
S
B
D

SONAR SIGNAL ACQUISITION AND
PROCESSING FOR IDENTIFICATION AND
CLASSIFICATION OF SHIP HULL FOULING

by

Professor A.J. Healey
Assistant Professor Ranjan Mukherjee
Principal Investigators

September 30, 1993

94-06015

‖‖‖‖‖‖‖‖‖‖‖‖‖‖‖‖‖‖

Best
Available
Copy

Naval Postgraduate School
Monterey, California

Real Admiral T. A. Mercer   H. Shull
Superintendent   Provost

This report was prepared in conjunction with research sponsored by the David Taylor Research Center, Annapolis, MD, and conducted at the Naval Postgraduate School.
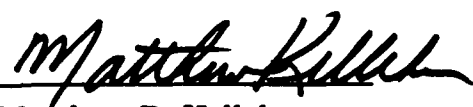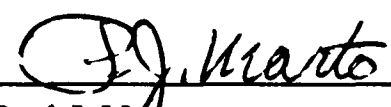
This report was prepared by:

_____

A. J. Healey
Professor of Mechanical Engineering

_____

Ranjan Mukherjee
Assistant Professor of Mechanical Engineering

Reviewed by: Released by:

_____   _____

Matthew D. Kelleher   Paul J. Marto
Chairman   Dean of Research
Dept. of Mechanical Engineering

REPORT DOCUMENTATION PAGE

1. AGENCY USE ONLY(Leave Blank)	2. REPORT DATE September 30 1993	3. REPORT TYPE AND DATES COVERED March 1 993 - Sept. 30 1993

4. TITLE AND SUBTITLE

SONAR SIGNAL ACQUISITION AND PROCESSING FOR IDENTIFICATION AND CLASSIFICATION OF SHIP HULL FOULING

5. FUNDING NUMBERS

6. AUTHOR(S)

A. J. Healey and R Mukherjee

7. PERFORMING ORGANIZATION NAME(S) AND ADDRESS(ES)

Naval Postgraduate School

Monterey, CA 93943-5000

8. PERFORMING ORGANIZATION REPORT NUMBER

NPS-ME-93-007

9. SPONSORING/MONITORING AGENCY NAME(S) AND ADDRESS(ES)

Naval Postgraduate School   and
Naval Surface Warfare Center
Annapolis Detachment, Annapolis, MD. 21402-5067

10. SPONSORING/MONITORING AGENCY REPORT NUMBER

11. SUPPLEMENTARY NOTES

The views expressed are those of the authors and do not reflectthe official policy or position of DOD or US Government.

12a. DISTRIBUTION/AVAILABILITY STATEMENT

Approved for public release: Distribution is unlimited

12b. DISTRIBUTION CODE

13. ABSTRACT *(Maximum 200 words)*

This work has involved the use of the Naval Postgraduate School's TRITECH ST 725 high frequency mechanically scanned sonar system to acquire sonar images of simulated surface roughness on an aluminum plate. Signal post processing for such image data is reviewed, and post processed data is analyzed and compared to the known roughness locations on the plate. The simulated roughness pattern of one half inch steel nuts is used as a preliminary experiment in the developemnt of a sonar detection system for marine growth on ship hull plating. Such a sonar system will be an integral part of any ship hull cleaning robot (SHACR). Contained in this report is a description of the experimental arrangement, typical sonar returns, a summary of image processing techniques, and results of processed data. The algorithms presented here will ultimately lead to a real time processing capability for the specification of location and extent of roughness as needed tfor the automatic direction of the robot's motion.

14. SUBJECT TERMS

Sonar Imaging, Robotics, Hull Cleaning, Autonomous Systems

15. NUMBER OF PAGES 34
16. PRICE CODE

17. SECURITY CLASSIFICATION OF REPORT UNCLASSIFIED	18. SECURITY CLASSIFICATION OF THIS PAGE UNCLASSIFIED	19. SECURITY CLASSIFICATION OF ABSTRACT UNCLASSIFIED	20. LIMITATION OF ABSTRACT SAR

ABSTRACT

This work has involved the use of the Naval Postgraduate School's TRITECH ST 725 high frequency mechanically scanned sonar system to acquire sonar images of simulated surface roughness on an aluminum plate. Signal post processing for such image data is reviewed, and processed data is analyzed and compared to the known roughness locations on the plate.

The simulated roughness (a pattern of one half inch steel nuts) is used in a preliminary experiment as part of the development of a sonar detection system for marine growth on ship hull plating. Such a sonar system will be an integral part of any Ship Hull Autonomous Cleaning Robot (**SHACR**).

Contained in this report is a description of the experimental arrangement, typical sonar returns, a summary of image processing techniques appropriate to this problem, and results of processed data as compared to the known locations of the simulated roughness.

The algorithms presented here will ultimately lead to a real time processing capability for the specification of location, extent, roughness level, as needed for the *automatic* direction of a **SHACR**'s motion control and cleaning systems.

i

TABLE OF CONTENTS

pg

ACKNOWLEDGMENT

LIST OF FIGURES

1.0 INTRODUCTION

Ship hull fouling is a common phenomenon having a strong impact on the Navy's operating costs. Fouling takes place through the growth of marine life, as in barnacles and grass, that increase the drag on the ship while it is motion. There is an attendant loss of efficiency and an increase in fuel consumption costs. On the other hand, cleaning fouled hulls is also expensive, and may require dry docking. In-situ cleaning without dry docking carries the risk of cleaning too deeply and releasing environmentally damaging deposits (and particularly copper) into the harbor.

A potentially cost saving, environmentally friendly, method of cleaning ship hulls involves the use of underwater robots equipped with sensors to detect and locate fouled sections of ship hull plating thereby selecting only the appropriate tools for the cleaning job which could change from area to area. Such a device would be useful as an aid to divers who currently have a difficult time in clearly identifying the location and extent of marine fouling underwater - even with the use of video cameras.

The purpose of this study was to initiate the development of sonar based sensory techniques for use with an autonomous underwater vehicle that will be

(1) able to better detect the extent of fouling on the hull of the ship, and,

(2) localize the areas of significant fouling

allowing *selective* cleaning to be put into effect.

In discussions with the sponsor, it was established early that visual sensing through video cameras would not be a generally useful technology because the murky waters of a harbor would prevent video images from being clearer than the current capability offers using divers.

The study has therefore focused on the use of high frequency imaging sonar as a device to detect and localize segments of fouling. In the following sections of this report, we will describe the particular sonar used, the example of an aluminum plate with simulated roughness, and the signal processing techniques available for use in converting data streams from the sonar head into signals that could be used to direct the movement of the cleaning robot.

While the study was funded at a very low level, the results do indicate that further investigations are warranted with the potential of reasonable success on real hulls. We strongly recommend that further experiments be conducted on plates that have realistic examples of marine fouling, followed by an experimental program to investigate hulls in situ.
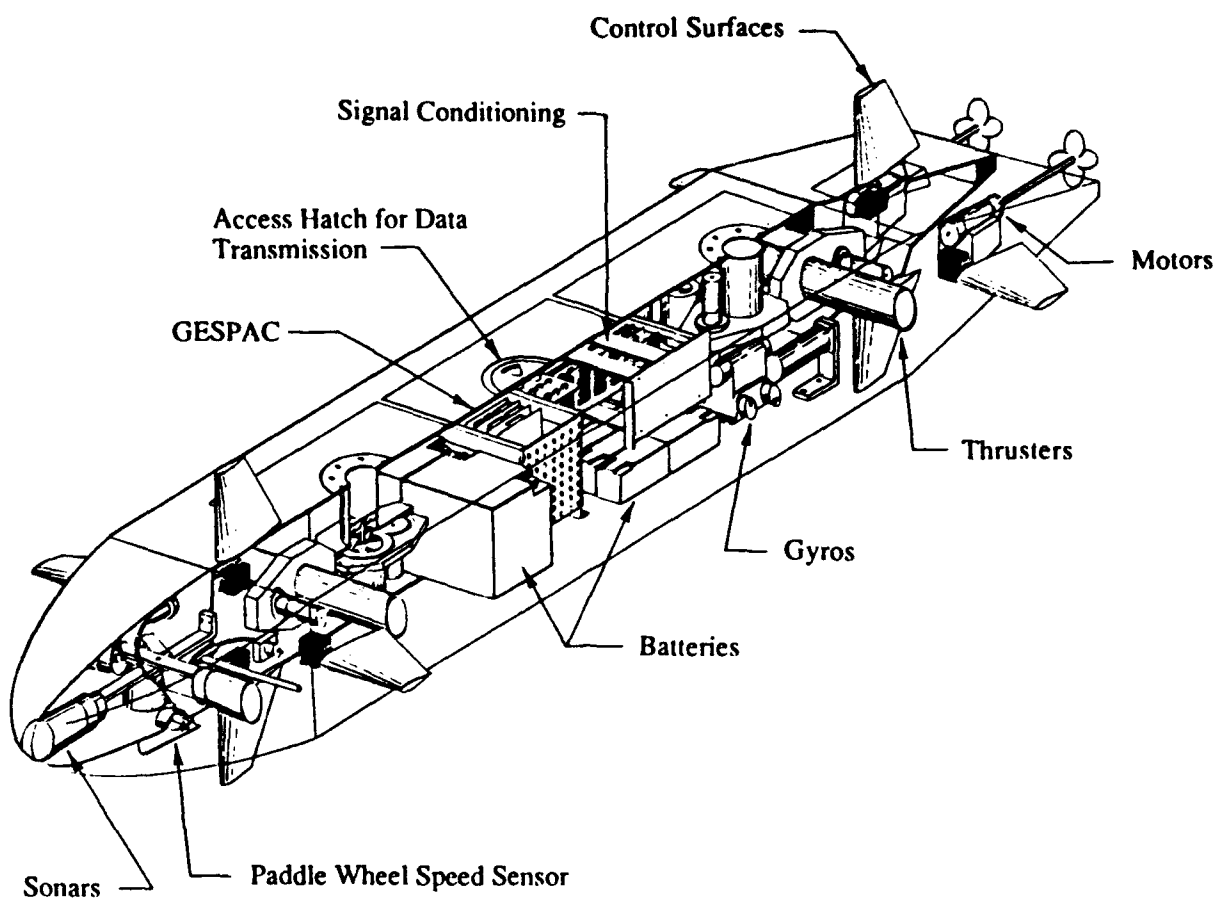
1

Control Surfaces

Signal Conditioning

Access Hatch for Data
Transmission

GESPAC

Motors

Thrusters

Gyros

Batteries

Sonars

Paddle Wheel Speed Sensor

Figure 1 Sketch of the NPS AUV II Autonomous Underwater Vehicle

2

2.0 THE TRITECH ST 725 SONAR

2.1   General

The use of high frequency sonars (to 1Megahertz) is expected to provide usable results for the imaging of marine fouling from barnacles and grass.

At the Naval Postgraduate School we have two TRITECH high frequency sonars. These are small units that fit into a small autonomous underwater vehicle - the NPS AUV II - shown in Figure 1. They would be suitable for installation on a **SHACR**, and this is one reason why interest in their use is strong.

The TRITECH ST 725 is a sector scanning sonar that is mechanically scannable through full 360 degrees rotation - or may be swept through any arbitrary defined sector given by starting and terminating angles. In sweeping through a defined sector, the sonar steps at 0.9 degrees per step at a rate of 20 steps per second, where at each step (bearing), a ping is emitted and the return is converted into an intensity (average power) value contained in each of several discrete segments of range called range bins. There are normally 128 range bins associated with the sonar returns from the ST 725 unit. The effective range associated with any bin is therefore 1/128 of the maximum range setting in use. One exception to this is when the maximum range setting of 6 m is used where it is divided into only 64 bins assoc)   ' with 600/64, or a discretization of 9.375 cm. for the shortest range setting. It follows .. for each bearing setting, a "scan line" is developed that provides a vector of intensity values - one for each range bin. The image processing problem is to convert the data so generated into meaningful metrics as the sonar sweeps over the plating of the ship hull. The metrics defined must be such that they will indicate the location and general degree of fouling.

The second sonar, the TRITECH ST 1000 is a one megahertz sonar with a one degree conical beam, mechanically scanned, where range for each bearing is based on time of flight of the first strong return. The data received at each bearing is therefore directly related to the distance from the sonar head to the object of the first return, and the ST 1000 thus becomes a useful profiling device.

As an example, Figure 2 shows a typical result of processing returns from the ST 725 sonar being set for a maximum range of 6 meters in the NPS Hovering Tank - a twenty foot square tank where the tank walls are clearly identified. In the basic configuration, the ST 725 communicates with a surface located PC computer with a VGA graphics screen to display the intensity results on a polar plot. The intensity of each pixel (a pixel is defined as the area of the screen occupied by a single range bin at a particular bearing step), is plotted in a color selected according to a color / intensity map.

However, while it is easy to see the sonar image on the PC screen, this mode of processing is unsuitable for the integration into a **SHACR** control system architecture. What is needed is the automatic identification of location and degree of fouled segments of the hull plating. The algorithms developed for that purpose would be the 'methods' of a Tactical Level Object in the context of the Tri-Level Software Architecture of the RBM, - a mission package controller - as proposed for the NPS AUV II, but which could be easily adapted to a **SHACR**. A large amount of work is still necessary to define the best methods which may be used in raising the level of autonomy in hull cleaning robots, although the results of studies of the kind performed here will certainly help.

Tritech Sonar Display

Range :   6 m   < Rings
Res   :   High   1.5 m
Scan   :   ON
Cont   :   OFF

Gain   :   35
Thresh :   10

Dirn   :   0
Sector :   60

Range :   6

Bearing: 30
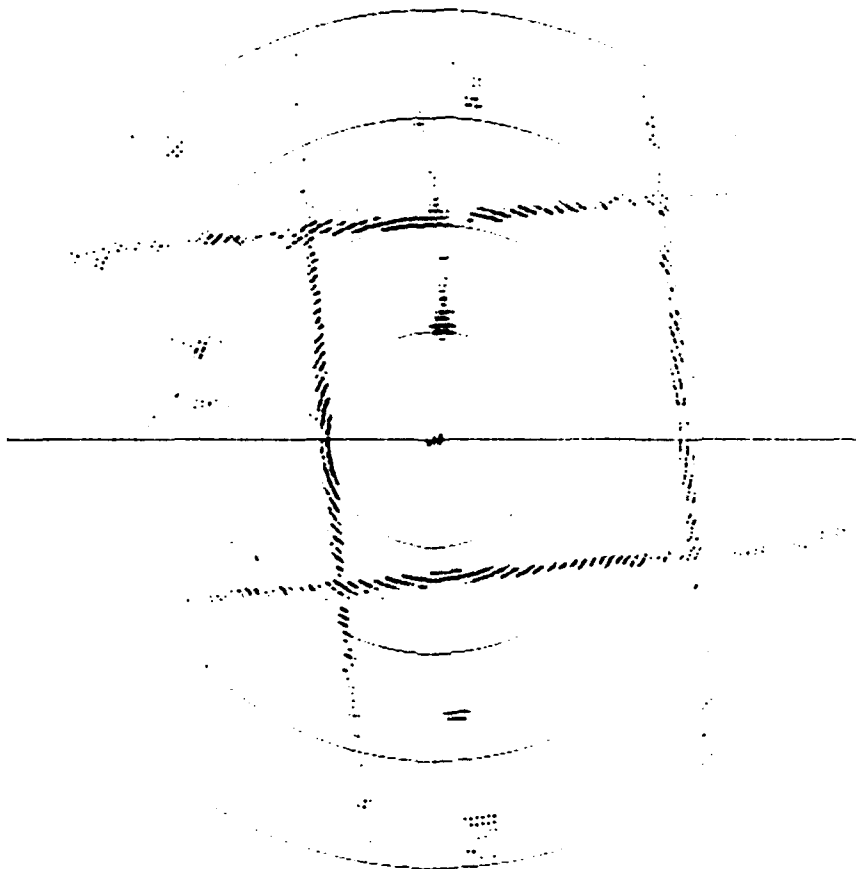
Figure 2 Typical Sonar Image Display from the ST 725 in the NPS Hover Tank

4

20 degrees

θ

24 degrees

1 2 3 4 5

Return rays

Intensity of returns differs for different range bins

Side View

Top View
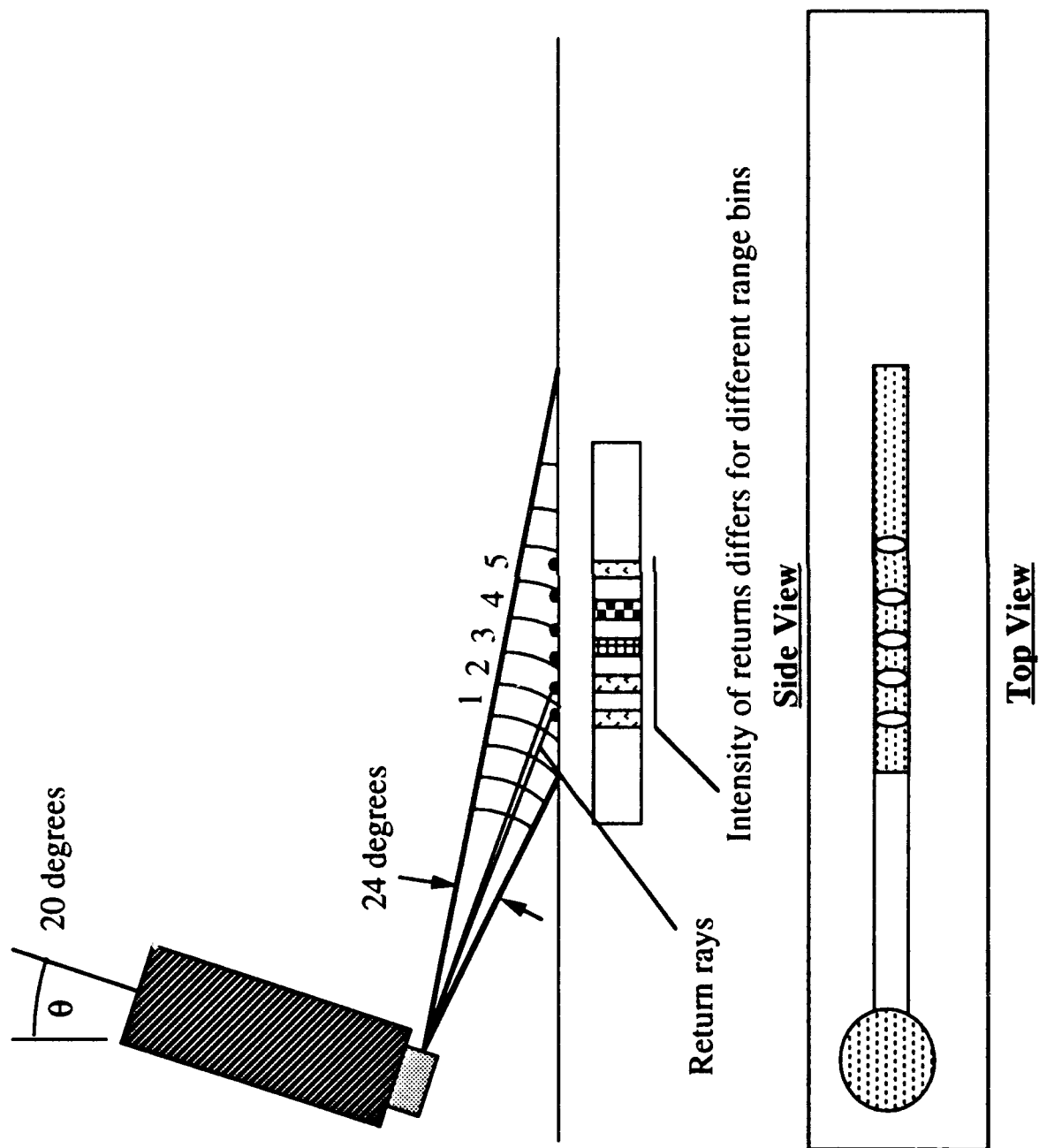
Figure 3   Geometry of the Experimental Arrangement

2.2 Modes of Operation

The ST 725 sonar can be set to have a maximum range at either 6, 10, 20, 25, 50, 75, or 100 meters. A gain setting is adjustable by the operator, and can be set so high that all returns are of the maximum intensity producing meaningless results if care in its setting has not been taken. For an appropriate gain setting - depending on the distance and conditions of the targeting - distinction can be made between returns from roughness and smooth segments of plating. The intensity of the returns are digitized into a scale of 1 - 15, where 15 represents the highest intensity of return. The sonar displays can be thresholded and controlled manually prior to display and the sweep speed can be either at 0.9 degrees per step, or, for low resolution but faster analysis, at 1.8 degrees per step.

2.3 Automatic Control of the ST 725 Sonar

We have been working - separately from this project - to automatically control the gain, threshold, sweeping sector, and sweep rate through ASCII commands sent to the serial port of the ST 725 sonar. Automatic control of the initialization process for the sonar has also been completed so that separate code - part of the execution level of the NPS AUV II control code will be able to direct the settings of the sonar and be able to read and process the returns. This work is soon to be available as a useful real time controller for the ST series of sonars.

3.0 IMAGE ACQUISITION CONCEPTS

3.1 General

Not the least part of the image acquisition problem is the arrangement of the sonar head in relation to the plate whose roughness characteristics are to be measured. Potentially there are a large number of configurations that could be used to acquire data representative of fouling. Two concepts have been considered.

For instance, a surface roughness profile could be measured using the ST 1000 as a vertical profilometer where the roughness of the plate surface would be the measure of the degree of fouling. Because of the resolution obtained with the least significant bit at the smallest range setting, the ST 1000 sonar would be expected to be accurate to about 2 cm. of height change . This was considered too coarse to be of primary interest to this application and it is concluded that a direct surface roughness measurement using this sonar is not sufficiently precise unless a special purpose sonar is developed.

Alternatively, using the ST 725 as a sector scanner the 24 degree high by 1 degree wide beam could be used to ensonify an area of the plate as it sweeps horizontally across the surface. Returns from the ensonified regions would then be distinguished by their intensities. While the resolution from the ST 725 would create pixels a little larger than the ultimately desired size (an unknown quantity at the present time) the horizontal arrangement appears to offer the most promise. The geometry for such a setup is illustrated in Figure 3.

3.2 Horizontal Configuration Detail

The side view in Figure 3 shows the sonar beam ensonifying a section of the plate with some roughness as modeled by the circles together with a return ray from the second object in the range bin marked as No. 2.

At the nominal range setting of 6 meters, there are 64 range bins and so the length of each range bin is

$$6/128 = 9.375 \text{ cm. per bin}$$

For a beam width of 1 degree, the beam width becomes

Bin Number	Range cm.	Width at End of Bin cm.
1	00.000 - 09.375	0.1636
2	09.375 - 18.750	0.3272
3	18.750 - 28.125	0.4909
4	28.125 - 37.500	0.6545
5	37.500 - 46.875	0.8181
6	46.875 - 56.25	0.9817
7	56.250 - 65.625	1.1453
8	65.625 - 75.000	1.3089
9	75.000 - 93.750	1.4726

7

Each sonar pixel is thus of radial length equal to 9.375 cm with a tangential width equal to the arc subtended by one degree at the appropriate radius from the sonar head. Average intensity of return from each sonar pixel is what is measured by the sonar

3.3　ST 725 Default Data Acquisition

The ST 725 Sonar is equipped with a software executable file running on an MS-DOS PC with a VGA Graphics screen capability that will process the returns from the sonar in real time - scanline by scanline and present the plots of intensity on a polar plot indicating Cartesian X-Y coordinates of the returns plotted. While this mode of operation is satisfactory for human operator visualization of the sonar returns, it is not suitable for consumption in real time by a **SHACR**.

3.4　Typical Data File Format

The sonar responds to commands that are issued through its serial port. A listing of possible commands includes:

1. Ping and process returns
2. Rotate one step (clockwise or counterclockwise)
3. Read serial port for processed return data
4. Initialize head to default settings
5. Set range, gain, resolution data

To generate an image, the sonar code that operates the head issues a series of commands that request the sonar to ping, process the returns, and take the next step. At this point, the returns data are written to a file which the user id asked to name, and displayed on the graphics screen for visualization.

Examination of the data file format has revealed that it is typically a large file in which - with some degree of compression by eliminating all data with intensity values equal to zero - the format of the data is as shown in the Table 1 below. What is clear from the form of the data in the Table 1 above is that each scanline is associated with a particular bearing angle. Within each scanline, non zero intensity readings are associated with range bins at various range values. By reading the PC file created by the default program, we are able to store such data and replot using the VAX system at NPS to produce a replica of the screen data produced by the default data processing. Replays of data taken in the NPS hovering tank where the ST 725 ensonifies the aluminum plate described later, are now given.

Figure 4 shows a typical sonar intensity map corresponding to a single sweep over a rough aluminum plate. The data is taken from a file created with a sonar gain setting of 11 and the data is plotted covering 2000 lines of data giving a sector sweep of an included angle of 90 degrees.

High points of intensity in the returns are shown in black while lower intensity returns are shown in colors nearer to white which corresponds to zero intensity. The series of figures in Figure 4 show the effects of gain setting and later, the effect of a low versus high resolution.

8

TABLE 1

Table of Typical Data

Data Line No.	Bearing Degrees	Range (cm)	Intensity Measure
1	-39.600000	0.000000	15
1	-39.600000	0.093750	9
1	-39.600000	0.187500	3
1	-39.600000	0.468750	8
1	-39.600000	0.562500	1
1	-39.600000	0.937500	1
1	-39.600000	1.031250	5
1	-39.600000	1.218750	8
1	-39.600000	1.312500	3
1	-39.600000	1.500000	6
1	-39.600000	1.593750	4
1	-39.600000	1.687500	7
1	-39.600000	1.781250	8
1	-39.600000	1.875000	6
1	-39.600000	1.968750	10
1	-39.600000	2.062500	2
1	-39.600000	2.156250	1
1	-39.600000	2.250000	3
1	-39.600000	2.343750	5
1	-39.600000	2.812500	3
1	-39.600000	2.906250	1
1	-39.600000	ა.750000	6
1	-39.600000	3.843750	7
1	-39.600000	4.218750	2
1	-39.600000	4.312500	10
1	-39.600000	4.406250	2
1	-39.600000	4.781250	4
1	-39.600000	4.968750	8
1	-39.600000	5.062500	4
1	-39.600000	5.250000	9
1	-39.600000	5.343750	4
1	-39.600000	5.812500	2
2	-38.700000	0.000000	15
2	-38.700000	0.093750	7
2	-38.700000	0.187500	2
2	-38.700000	0.468750	3
2	-38.700000	0.937500	1
2	-38.700000	1.031250	6
2	-38.700000	1.125000	5
2	-38.700000	1.218750	7
2	-38.700000	1.312500	6
2	-38.700000	1.406250	8
2	-38.700000	1.500000	4

Tritech Sonar Display

Range :   5 m   < Rings

Res   :   High   1.5 m

Scan :   ON

Cont :   OFF

Gain   : 11

Thresh : 10

Dirn   :   0

Sector : 60

Range :   5

Bearing: 90

Figure 4a Typical Sonar Intensity Map

10

Tritech Sonar Display

Range :   3 m   ‹ Rings
Res   :   High   1.5 m
Scan :   ON
Cont :   OFF

Gain   : 11
Thresh : 10

Dirn   : 0
Sector : 60

Range : 3
Bearing: 30

Threshold = 12:   Gain = 11
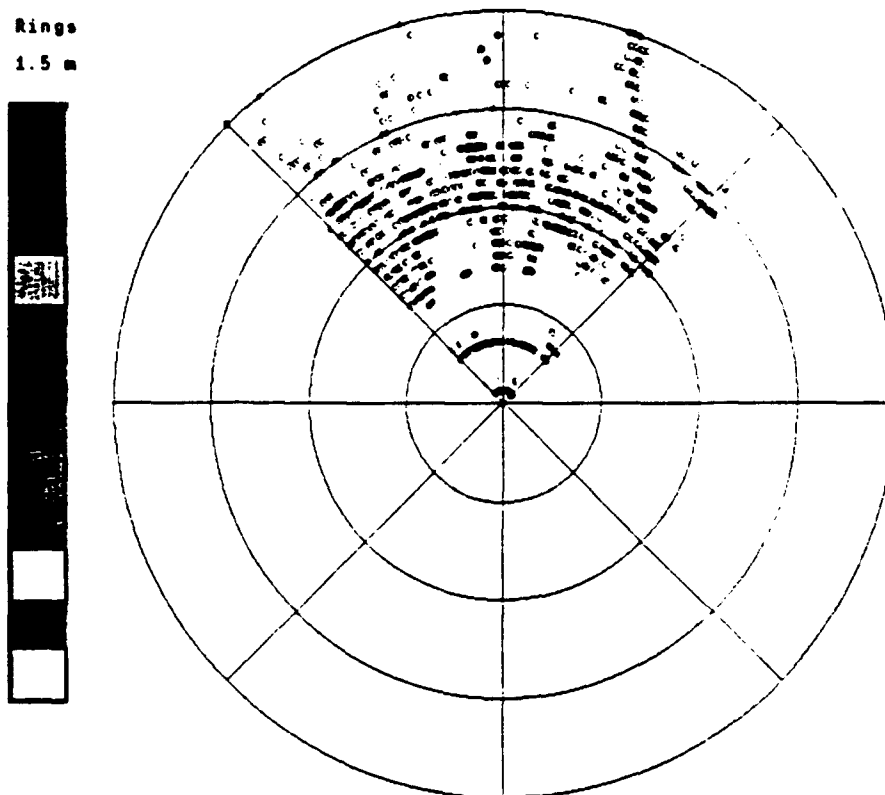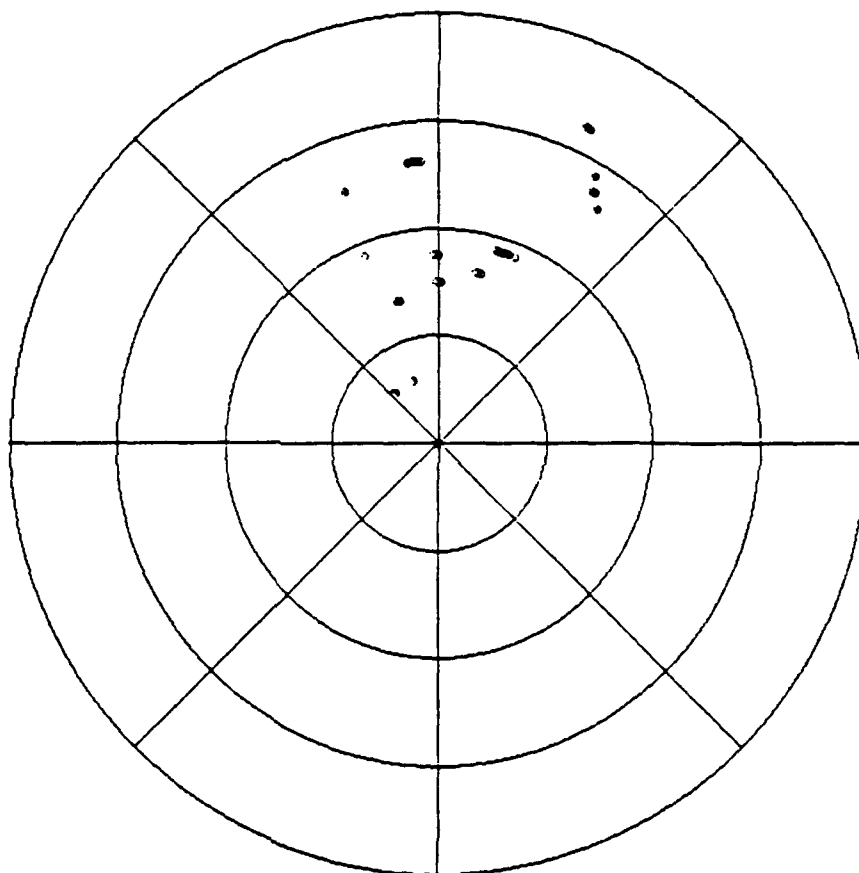
Figure 4b Typical Sonar Intensity Map

11

Tritech Sonar Display

Range :   3 m   < Rings
Res   :   High   1.5 m
Scan :   ON
Cont :   OFF

Gain   : 11
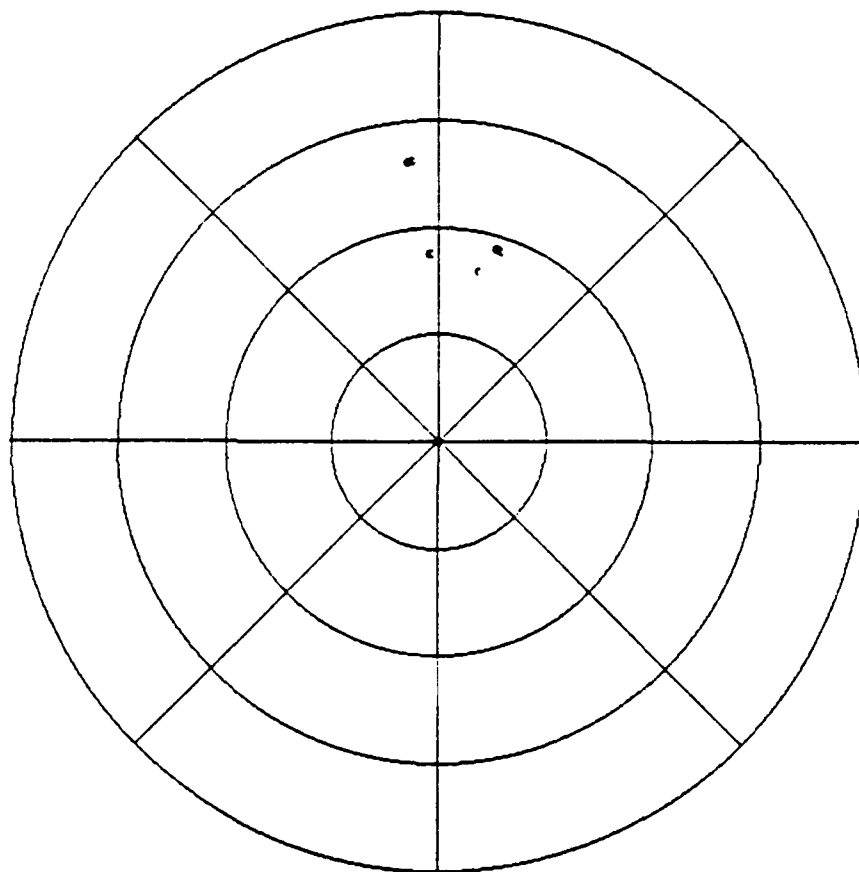Thresh : 10

Dirn   : 0
Sector : 60

Range : 3
Bearing: 30

Threshold = 15   Gain =11

Figure 4c Typical Sonar Intensity Map

12

4. SONAR SIGNAL PROCESSING

4.1 Introduction

Sonar signal processing may be subdivided into a four principal areas: (a) Preprocessing, (b) Segmentation, (c) Description, and (d) Interpretation. Preprocessing deals with techniques such as noise reduction and enhancement of details. Segmentation is the process that partitions an image into objects of interest. Description deals with the computation of features like size, shape, etc., suitable for differentiating one object from another. Finally, interpretation assigns meaning to an ensemble of recognized objects. In our case where we take sonar images of the fouled hull of a ship, the data will be interpreted to assess the location and extent of fouling. In the next sections we describe in brief the methods of preprocessing, segmentation, description, and interpretation of sonar images.

4.2 Preprocessing of data from the sonar

Preprocessing may be considered as a low-level imaging process that is primitive in the sense that it requires no intelligence. It will take us from the image formation process to the compensations such as noise reduction, and finally to the extraction of primitive image features such as intensity discontinuities.

There are two basic approaches to preprocessing: the spatial domain methods, and the frequency domain methods via the Fourier transform. The spatial domain refers to the aggregate of pixels composing an image and the spatial domain methods are procedures that operate directly on these pixels. Preprocessing functions in the spatial domain may be expressed as

$$g(x, y) = h[f(x, y)] \tag{1}$$

where, $f(x, y)$ is the input image, $g(x, y)$ is the preprocessed image, and h is an operator on f, defined over some neighborhood of (x, y). The principal approach used in defining a neighborhood about (x, y) is to use a square or rectangular subimage area centered at (x, y) as shown in Fig.4.

One of the spatial domain methods used most frequently is based on the use of so-called convolution masks (also referred to as templates, windows, or filters). Basically, a mask is a 2-D array (e.g. 3 × 3), such as the one shown in Fig.4, whose coefficients are chosen to detect a given property in an image. As shown in Fig.5, if we let $w_1, w_2, \cdots, w_9$ represent mask coefficients and consider the 8 neighbours of (x, y), we may perform the following operation

$$h\left[f(x,y)\right] = w_1\,f(x-1,y-1) + w_2\,f(x-1,y) + w_3\,f(x-1,y+1)$$

$$+ w_4\,f(x,y-1) + w_5\,f(x,y) + w_6\,f(x,y+1)$$

$$+ w_7\,f(x+1,y-1) + w_8\,f(x+1,y) + w_9\,f(x+1,y+1) \tag{2}$$

The frequency domain refers to the aggregate of complex pixels resulting from taking the Fourier transform of an image. Due to the extensive processing requirements, frequency domain methods are not nearly as widely used as are spatial domain methods.

In the next subsections we discuss the methods of image preprocessing that we will use in the next part of this project.

4.2.1 Smoothing

Smoothing operations are used for reducing noise and other spurious effects that may be present in an image as a result of sampling, quantization, transmission, or disturbances in the environment during image acquisition. In our case, we have observed that the data acquired by the sonars have a significant amount of noise that may have resulted from multiple reflections of the sonar signal.

Neighborhood Averaging   Neighborhood averaging is a straightforward spatial domain technique used for image smoothing. Given an image $f(x,y)$. the procedure is to generate a smooth image $g(x,y)$ whose intensity at every point (x,y) is obtained by averaging the intensity values of the pixels of f contained in a predefined neighborhood of (x,y). In other words, the smoothed image is obtained by using the relation

$$g(x,y) = \frac{1}{P} \sum_{(n,m)\in S} f(n,m) \tag{3}$$

for all x and y in $f(x,y)$. S is the set of coordinates of all points in the neighborhood of (x,y), including (x,y) itself, and P is the total number of points in the neighborhood.

Median Filtering   One of the principal difficulties in neighborhood averaging is that it blurs images and other sharp details. The blurring can often be reduced significantly by the use of so-called median filters, in which we replace the intensity of each pixel by the median of the intensities in a predefined neighborhood of that pixel, instead of by the average. A principal function of the median filtering is to force functions with very distinct intensities to be more like their neighbors, thus actually eliminating spikes that appear isolated in the area of the filter mask.

Image Averaging   Consider a noisy image $g(x,y)$ which is formed by the addition of noise $n(x,y)$ to an uncorrupted image $f(x,y)$, that is

$$g(x,y) = f(x,y) + n(x,y) \tag{4}$$

where, it is assumed that the noise is uncorrelated and has zero average value. The objective of this procedure is to obtain a smoothed result by adding a given set of noisy images. $g_i(x,y), i = 1, 2, \cdots, K$. If the noise satisfies the assumptions stated above, the it can be shown that if the image $\bar{g}(x,y)$ is formed by averaging K different noisy images,

$$\bar{g}(x,y) = \frac{1}{K} \sum_{i=1}^{K} g_i(x,y) \tag{5}$$

it follows that

$$E\{\bar{g}(x,y)\} = f(x,y) \tag{6}$$

and

$$\sigma_{\bar{g}}^2(x,y) = \frac{1}{K} \sigma_n^2(x,y) \tag{7}$$

where, $E\{\bar{g}(x,y)\}$ is the expected value of $\bar{g}$, and $\sigma_{\bar{g}}^2(x,y)$ and $\sigma_n^2(x,y)$ are the variances of $\bar{g}$ and n, all at coordinates (x,y). Since $E\{\bar{g}(x,y)\} = f(x,y)$, this means that $\bar{g}(x,y)$ will approach the uncorrupted image $f(x,y)$ as the number of noisy images used in the averaging process increases.

4.2.2 Enhancement

Image enhancement is a major area in image processing and much of the success of the subsequent processing algorithms is dependent upon it. Our ability to accurately predict the areas of fouling on the hull of the ship and the extent of the fouling will depend upon the enhancement procedures.

Histogram Equalization   Let the variable r represent the intensity of pixels in an image to be enhanced. It will be assumed initially that r is a normalized, discrete variable lying in the range $0 \leq r \leq 1$. For r lying in this range, attention will be focussed on transformations of the form

$$s = T(r) \tag{8}$$

which produce an intensity value s for every pixel value r in the input image. It is assumed that the transformation satisfies the conditions:

1. T(r) is single-valued and monotonically increasing in the interval $0 \leq T(r) \leq 1$.

2. $0 \leq T(r) \leq 1$ for $0 \leq r \leq 1$.

Condition 1 preserves the order from black to white in the intensity scale, and condition 2 guarantees a mapping that is consistent with the allowed 0 to 1 range of pixel values. The probabilities are given by the relations

$$p_r(r_k) = \frac{n_k}{n}, \qquad 0 \le r \le 1$$
$$k = 0, 1, \cdots, L - 1 \qquad (9)$$

where L is the number of discrete intensity levels, $p_r(r_k)$ is an estimate of the probability of intensity r_k, n_k is the number of times this intensity appears in the image, and n is the total number of pixels in the image. A plot of $p_r(r_k)$ versus r_k is usually called a histogram, and the technique used for obtaining a uniform histogram is known as histogram equalization of histogram linearization. Equation (8) in the discrete form is given by

$$s_k = T(r_k) = \sum_{j=0}^{k} \frac{n_j}{n}$$
$$= \sum_{j=0}^{k} p_r(r_j) \qquad (10)$$

for $0 \le r_k \le 1$, and $k = 0, 1, \cdots, L - 1$. It is noted that to obtain the mapped value s_k corresponding to r_k, we simply sum the histogram components from 0 to r_k.

Local enhancement   The histogram equalization procedure is global in the sense that pixels are modified by a transformation function which is based on the intensity distribution of an entire image. While this global approach is suitable for overall enhancement, it is often necessary to enhance details over small areas.

The histogram processing techniques are easily adaptable to local enhancement. The procedure is to define an $n \times m$ neighborhood and move the center of this area from pixel to pixel. At each location we compute the histogram of the $n \times m$ points in the neighborhood and obtain a histogram equalization function. The function is finally used to map the intensity of the pixel centered in the neighborhood. The center of the $n \times m$ region is then moved to an adjacent pixel location and the procedure is repeated.

4.2.3 Thresholding

Image thresholding is one of the principal techniques used for object detection, especially in applications requiring high data throughput.

Suppose that the image $f(x, y)$ is composed of a light object on a dark background, such that object and background pixels are grouped into two dominant modes. One obvious way to extract the objects from the background is to select a threshold T which separates

16

the intensity modes. Them, any point (x, y) for which $f(x, y) > T$ is called an object point, otherwise the object is called a background. In the case where the image has three dominant modes, we can use the same approach and classify a point (x, y) as belonging to one object class if $T_1 \le f(x, y) \le T_2$, to the other object class if $f(x, y) > T_2$, and to the background if $f(x, y) \le T_1$. Based on the foregoing concepts, we may view thresholding as an operation that involves tests against a function T of the form

$$T = T[x, y, p(x, y), f(x, y)] \tag{11}$$

where $f(x, y)$ is the intensity of point (x, y), and $p(x, y)$ denotes some local property of this point, for example the average intensity of a neighborhood centered at (x, y). We create a thresholded image $g(x, y)$ by defining

$$g(x, y) = \begin{cases} 1 & \text{if } f(x, y) > T \\ 0 & \text{if } f(x, y) \le T \end{cases} \tag{12}$$

Thus in examining $g(x, y)$, we find that pixels labeled 1 correspond to objects, while pixels labeled 0 correspond to the background.

When T depends only on $f(x, y)$, the threshold is called global. If T depends both on $f(x, y)$ and $p(x, y)$, then the threshold is called local.

4.3 Region-Oriented Segmentation

The objective of segmentation is to partition an image into regions. In our case, we are interested in segregating areas on the hull of the ship that need to be cleaned due to excessive fouling. Such areas will be identified from the images obtained using the sonars.

Let R represent the entire image region. We may view segmentation as a process that partitions R into n subregions, $R_1, R_2, \cdots, R_n$, such that

1. $\cup_{i=1}^{n} R_i = R$

2. R_i is a connected region, $i = 1, 2, \cdots, n.$

3. $R_i \cap R_j = \phi$ for all i and j, $i \ne j$

4. $P(R_i) = \text{TRUE}$ for $i = 1, 2, \cdots, n$

5. $P(R_i \cap R_j) = \text{FALSE}$ for $i \ne j$

where $P(R_i)$ is a logical predicate defined over the points in set R_i, and ϕ is the null set.

Condition 1 requires that the segmentation must be complete; that is, every pixel must be in a region. The second condition requires that points in a region must be connected. Condition 3 indicates that regions must be disjoint. Condition 4 deals with the properties that must be satisfied by the pixels in a segmented region. Finally, condition 5 indicates that regions R_i and R_j are different in the sense of predicate P.

Region growing by pixel aggregation   We will start with a set of "seed" points and from these grow regions by appending to each seed point those neighboring pixels that have similar properties like intensity. The property that we will use to include a pixel in a region will be based on the absolute difference between the intensity of the seed and a threshold value T.

Region splitting and merging   The procedure discussed above grows regions starting from a given set of seed points. An alternative is to subdivide an image into a set of arbitrary, disjoint regions and then merge or split the regions in an attempt to satisfy the conditions stated at the beginning of the section. A split and merge algorithm may be explained as follows

Let R represent the entire image, and select a predicate P. Assuming a square image, one approach for segmenting R is to successively subdivide it into smaller and smaller quadrant regions such that, for any region R_i, $P(R_i) =$ TRUE. The procedure starts with an entire region R. If $P(R)$ is FALSE, we divide the image into quadrants. If $P(R)$ is FALSE for any quadrant we divide that quadrant into subquadrants and so on. This particular splitting technique has a convinient representation in the form of a so-called "quadtree" (i.e. a tree in which each node has exactly four descendants). A simple illustration is shown in Fig.3. It is noted that the root of the tree corresponds to the entire image and that each node corresponds to a subdivision.

If we used only splitting, it is likely that the final partition would contain adjacent regions with identical properties. This may be remedied by allowing merging, as well as splitting. In order to satisfy the segmentation conditions stated earlier, we merge only adjacent regions R_i and R_j only if $=$ TRUE.

The preceding discussion may be summarized by the following procedure in which, at any step, we

1. Split into four disjoint quadrants any region R_i for which $P(R_i) =$ FALSE.

2. Merge any adjacent regions R_j and R_k for which $P(R_j \cup R_k) =$ TRUE.

3. Stop when no further merging or splitting is possible.

4.4 Description of the sonar image

Description deals with the computation of features like size, shape, etc., suitable for differentiating one object from another in the image. In our case, we are interested in identifying clusters of fouled areas and identify the size and shape of these clusters.

Some simple descriptors   A number of existing imaging systems are based on regional descriptors which are rather simple in nature. The area of a region is defined as the number

of pixels contained within its boundary. The major and minor axes of a region are useful for establishing the orientation of an object. The ratio of the lengths of these axes, called the eccentricity, is also a global descriptor of the shape. The perimeter of a region is the length of its boundary. Although the perimeter is sometimes used as a descriptor, its most frequent application is in establishing a measure of compactness of a region, defined as $perimeter^2/area$.

Image description   While there are many ways to describe an image, we will primarily be interested in the intensity distribution over a connected region in the image. The simple regional descriptors will provide us with the shape and size of the connected region. Subsequently, we will use the first and the second moments of the intensities of every pixel in the connected region from some fixed reference point to obtain the mean and the standard deviation. These quantities will characterize the intensity distribution over the entire connected region and will be used to differentiate one connected region from another in the extent of fouling.
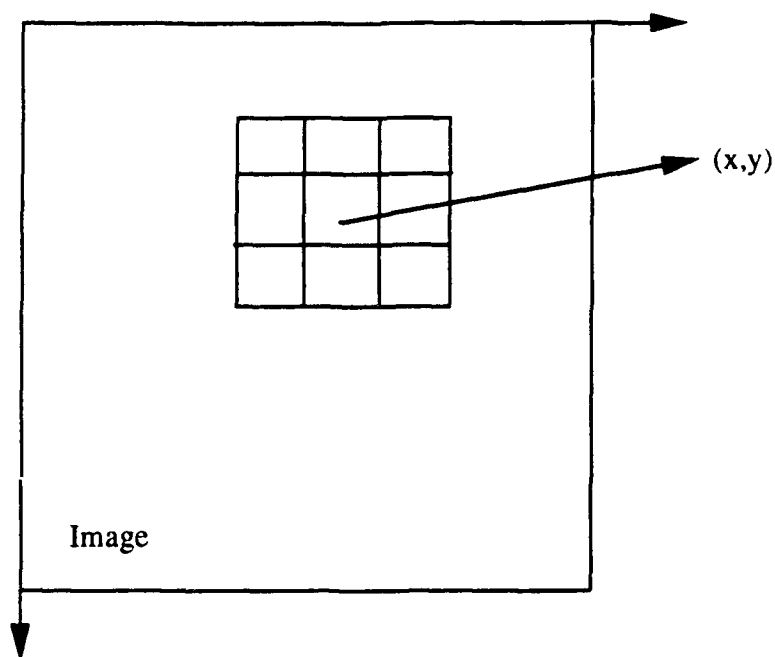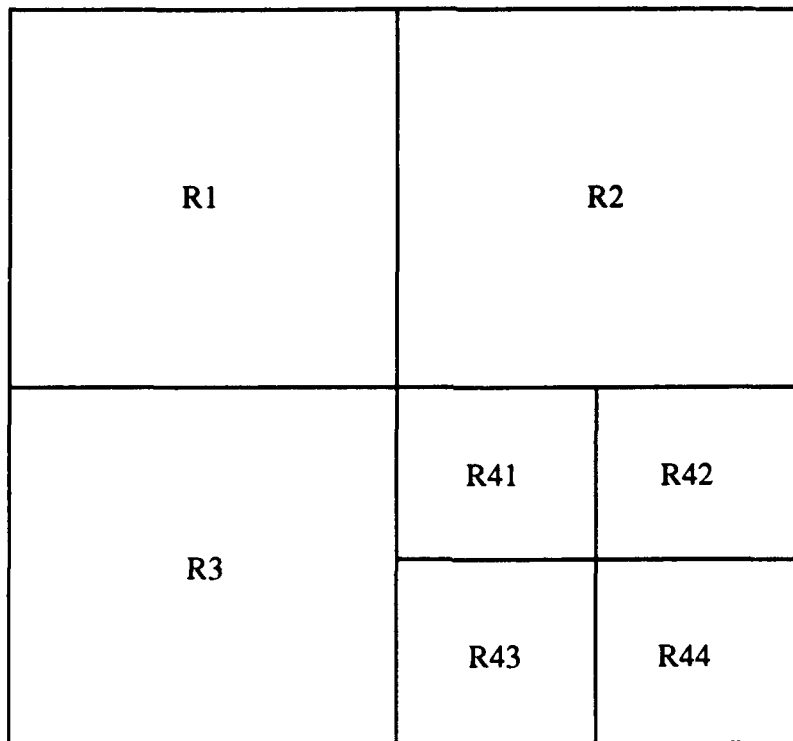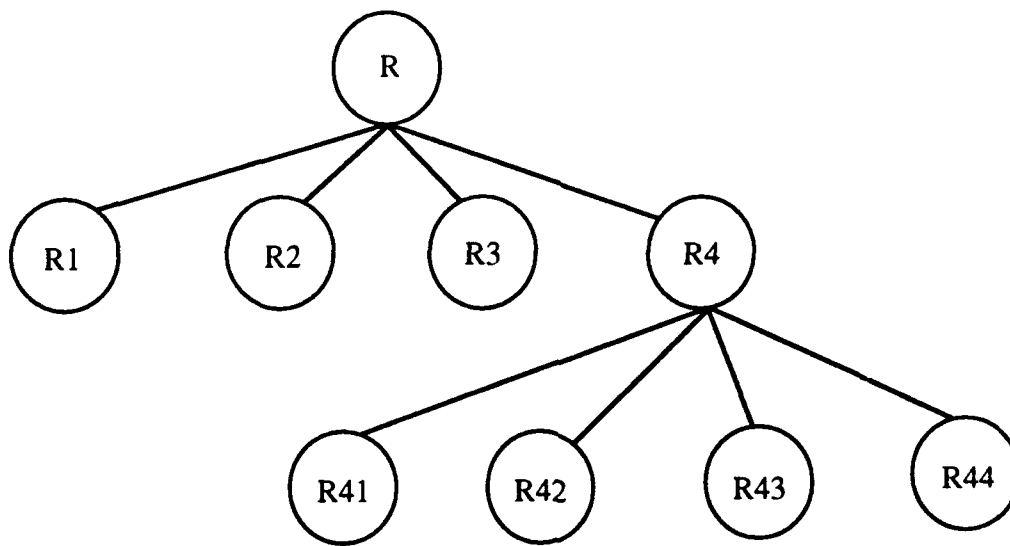
Figure 5. A 3 X 3 neighborhood about a point (x, y) in an image

w1 (x-1, y-1)	w2 (x-1, y)	w3 (x-1, y+1)
w4 (x, y-1)	w5 (x, y)	w6 (x, y+1)
w7 (x+1, y-1)	w8 (x+1, y)	w9 (x+1, y+1)

Figure 6. A general 3 X 3 mask showing coefficients and
corresponding image pixel locations

(a)

(b)

Figure 7. (a) Partitioned Image, (b) Corresponding quadtree

5.0 EXPERIMENTS WITH THE ALUMINUM PLATE

5.1   General

The dimensions of the test plate used for this study are shown in Figure 8. Figure 6 shows the geometry for the test setup and the relationships between slant range and horizontal range for the testing configuration. Analysis of the geometry of Figure 9 would indicate that if θ is the elevation angle of the sonar head and the sweep azimuth angle is ψ, then the horizontal coordinates of a slant range vector r, in global plate coordinates [X,Y,Z] would be

$$X = r\cos\theta\cos\psi$$
$$Y = r\sin\psi$$
$$Z = -r\sin\theta\cos\psi$$

In this transformation there is a question concerning the value to use for the angle θ. Because the beam has a height of 24 degrees, and knowing that θ is a nominal say 20 degrees means that the particular return could be associated with 20 plus or minus $\theta/2$. However, since we are assuming that the return is also associated with the plane of the plate, we are able to compute θ in terms of the particular slant range value, r, and the height value, h. It follows that

$$\cos\theta = \sqrt{1 - \left(\frac{h}{r}\right)^2}$$

with an uncertainty associated with the length of the bin size.

5.2   Experimental Data Files Obtained

For the experimental work, three basic data files were obtained by sweeping over the plate with the sonar set at different gains and both low and high resolution conditions. Too high a gain setting would result in filling the screen with white dots while too low a gain setting would not give a registration of the roughness to be identified. The high / low resolution settings essentially showed that high resolution would be needed. The data files were labeled as

scan_pal_11h.d
scan_pal_11l.d
scan_pal_5h.d

The number 11 or 5 refers to the sonar gain setting and the designation l or h refers to the resolution of the data to be either low or high.

The data from the files have been analyzed by thresholding, plotting on Cartesian coordinates, contour plotted, and, algorithms have been developed for automatic identification of the mean range to a high spot as well as effective size of a region of high returns.
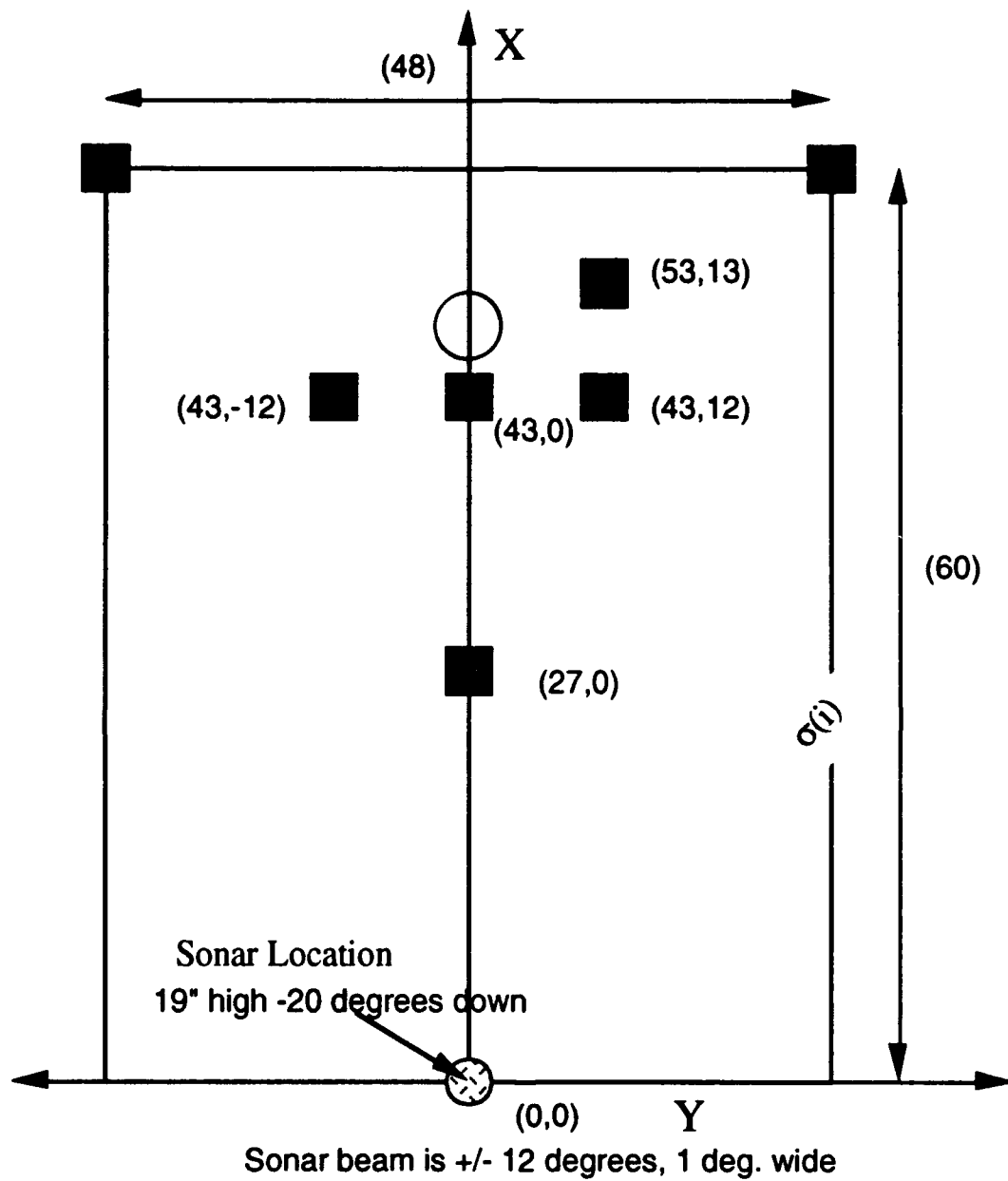
Figure 8   Dimensions of the Aluminum Test Plate Used for this Study and the Locations of the Nuts (All Dimensions in Inches)
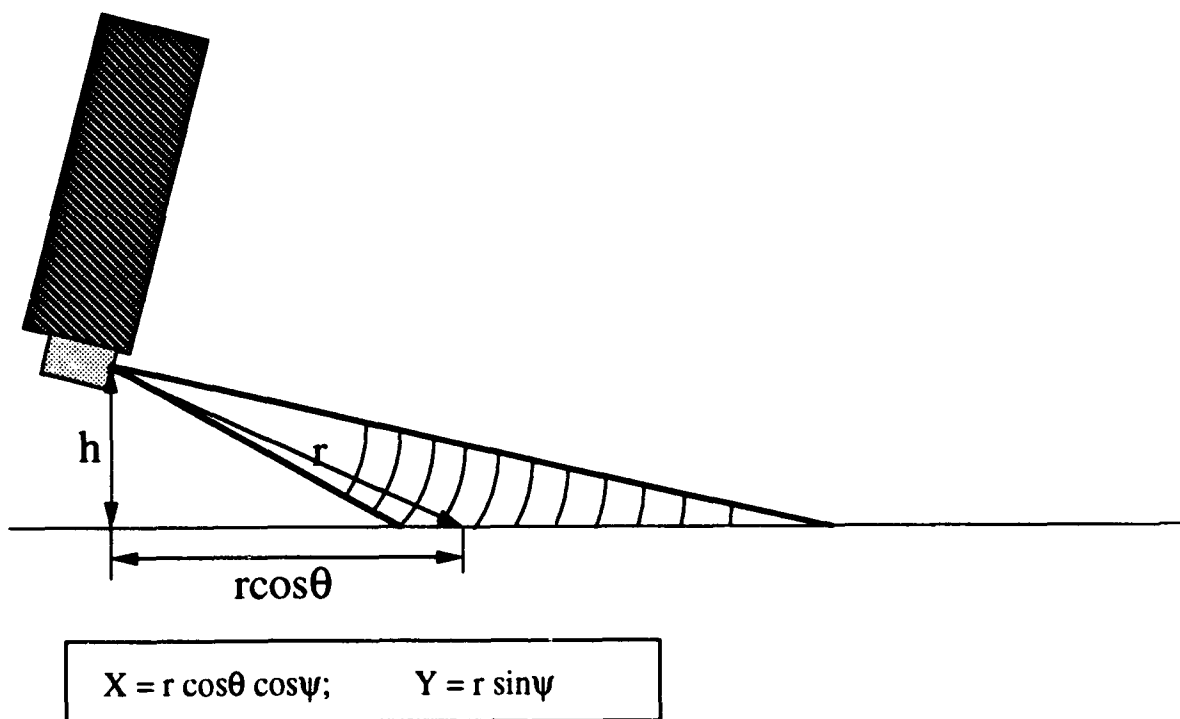
$$X = r \cos\theta \cos\psi; \qquad Y = r \sin\psi$$

Figure 9 Transformations from Slant Range to Plate Plane Coordinates

6.0 RESULTS OF CARTESIAN REPRESENTATION OF THRESHOLDED RETURNS

6.1 General

Since the results are contained in the values of the intensity, it is most convenient to develop the data set in terms of vector valued quantities where they are entries in a row column matrix. Intensity values are thus viewed as the entries in the matrix Z (i, j):

$$I = Z(i, j);$$

The index i, corresponds to the bearing where 1 represents the initial heading of the sonar and the highest value represents the bearing as scan number increases. There is clearly a mapping between i and the heading in degrees. Similarly, there is a mapping between j and the range. j is the bin number and, in this case, takes on values from 0 to 64. The mapping between j and the range in cm. is given as previously noted.

With a view from Figure 3 of the geometry of the setup, we convert the slant range data into equivalent x, y, coordinates for comparison with the Cartesian plate coordinates of simulated fouling sections.

The result is shown in Figure 10. Figure 10 contains the locations in plate coordinates of the nuts that were used to simulate discrete fouling, and, superimposed are the sonar returns in the thresholded bands T=12 - 15;

Since there is a discretization on slant range of $\sigma^{(i)}$ $\smile$ /5 cm. and an angle resolution of +/- 1 degrees arc, it is apparent that there are indeed returns that would be useful to work with, even though the returns do not lie precisely on the locations of the nuts. The overall result is quite remarkable however, and is very encouraging.

Lower intensity returns are found over a large area as shown in Figure 11 which, for example shows returns in the range of intensities from 7 - 11.

A contour plot of the matrix Z with thresholded returns between T=[12,15], is shown in Figure 12. Here, again, it is clear that the sonar is able to detect areas of simulated roughness. The contour plot capability of the **MATLAB** software package has been used to produce the Figures for these results.

6.2 Effects of Thresholding

Thresholding the data may be done to eliminate the confusion cause by massive amounts of low intensity data. Use of an upper threshold is sometimes useful if areas of high intensity need to be leveled for the purpose of computing size of the high intensity zones.

To threshold the data, the following algorithm is used.

```
for i=1,m
for j=1,l
if Z(i,j)<T_lower, Z(i,j) = T_lower;
if Z(i,j)> T_upper, Z(i,j) = T_upper
```
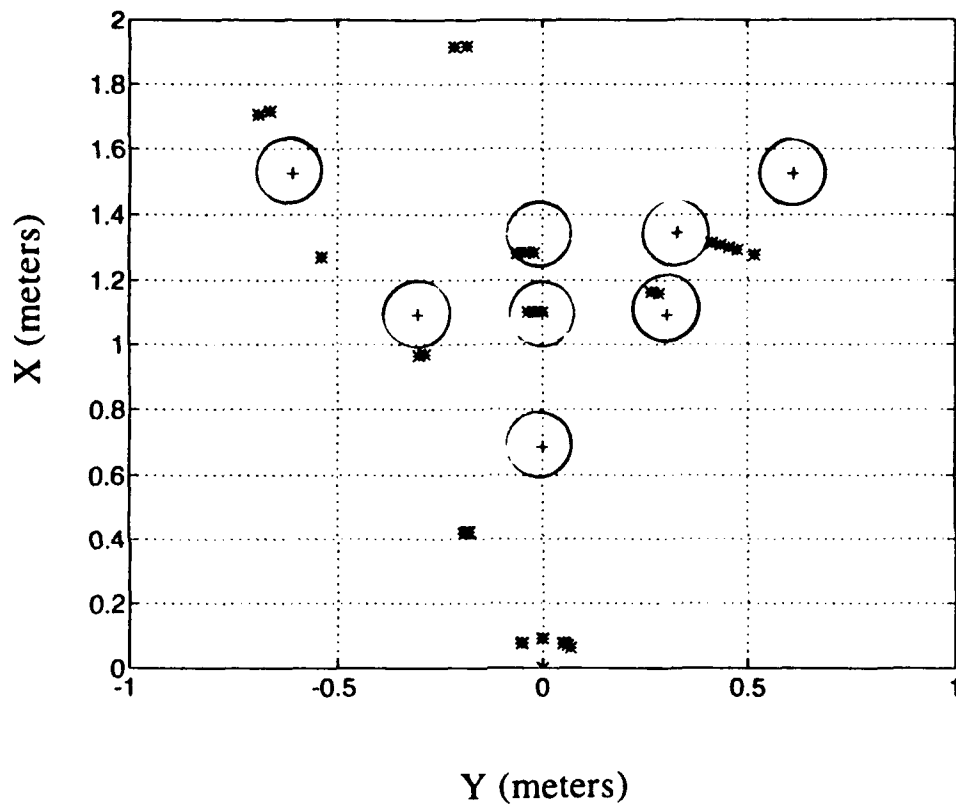
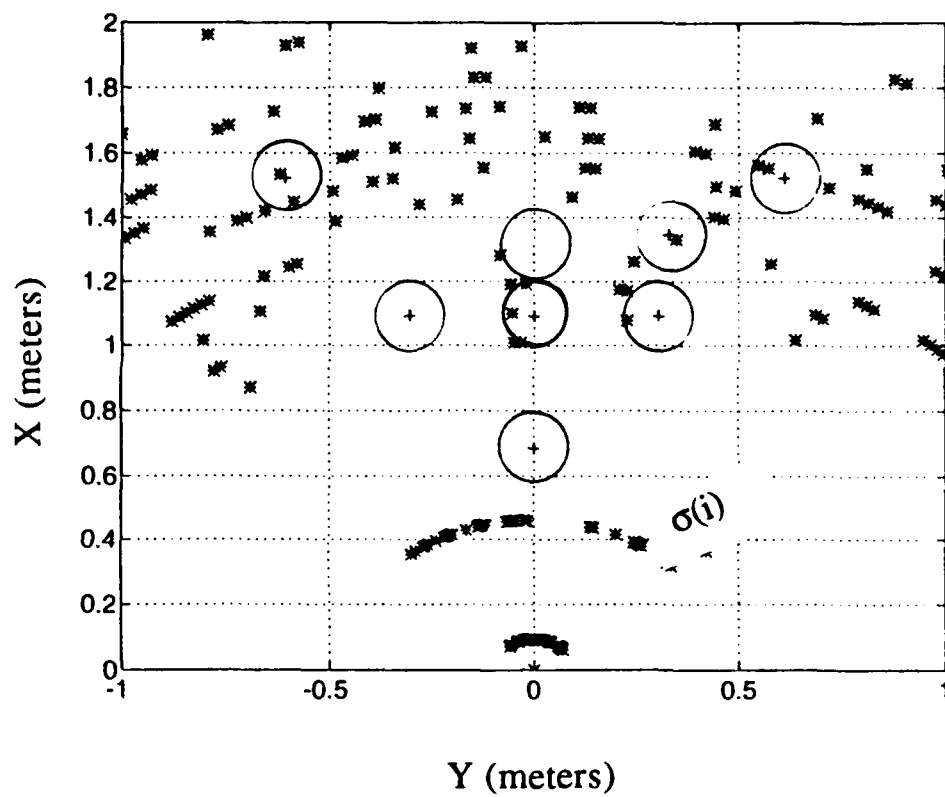Figure 10 Returns in the Range 12-15 Superimposed on the Simulated Roughness
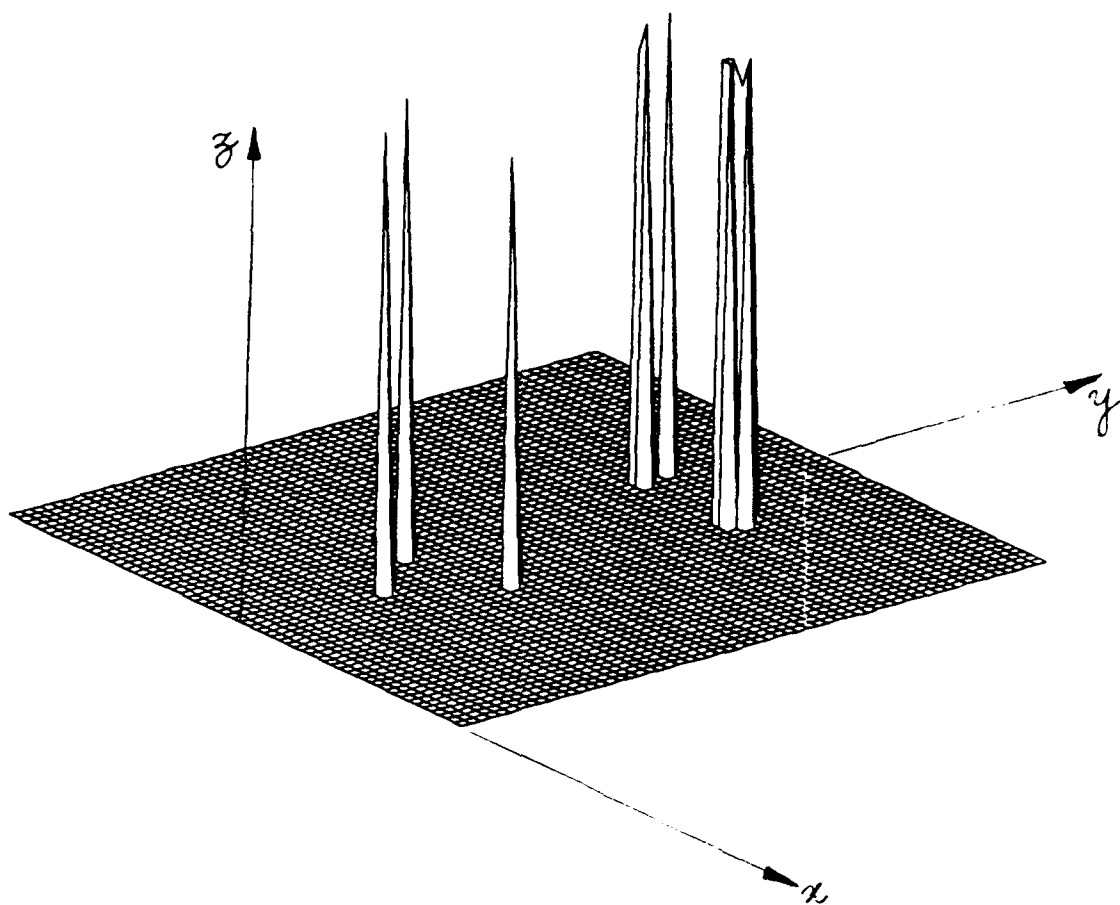
Figure 11 Returns in the Range 7 - 11 Intensity

Figure 12. Contour plot of the intensity matrix **Z**.

where T_{upper} and T_{lower} are the upper and lower thresholds used and m and l are the array sizes for the number of bearings and range bins.

6.3 Real Time Data Scan Line Processing

In view of the above, it would seem that processing the sonar returns after data acquisition could be done, displaying the results for the robot user, but, on the other hand, with a certain amount of on board processing, an estimation of the location and severity of the fouling is really needed in real time. In other words, examination of the matrix Z (i, j), reveals that using the intensity weighted centroid computation would yield the mean distance s0 and hence, using the bearing information, the mean locations x0, y0, in plate coordinates could be computed automatically.

6.3.1 Mean Range Algorithm

Under the assumption that the intensity / range along a scanline is unimodal, we can find the mean range by the first moment of intensity. That is, an intensity weighted mean range will give a measure to the 'centroid' of the intensity versus range plot. This computation is applied scan by scan and is performed by the following code.

```
for i=1,m
r0(i)=r*Z(i,:)/(sum(Z(i,:));
end;
```

where $r_0(i)$ represents the mean range along scan line i for a t $\sigma^{(i)}$ number of m bearings.

6.3.2 Depth Estimation Algorithm

A measure of the depth extent of the segments of strong returns along a scan line can be found by the second moment of intensity, and, having established values for r0(i), we find that, if $\sigma(i)$ is viewed as the standard deviation of intensity weighted variations from the mean range, then the algorithm is as follows.

```
for i=1,m
σ2(i)=(r-r0(i)*ones(size(r)).^2*Z(i,:) / (sum(Z(i,:));
σ(i)=sqrt(σ2(i));
end;
```

In the above, .^2 refers to the element by element square of the vector of range differences from the mean range for that bearing.

6.3.3 Mean Strength Algorithm

The mean strength of returns contained within the area of the assumed unimodal high strength zone is also an interesting metric and is found by averaging the intensity values contain inside the ranges defined by $(r_0(i) - \sigma(i))$ and $(r_0(i) + \sigma(i))$. We call this metric, the mean strength (mst(i)).

Such a computation yields the result shown in Figure 13. Notice that the locations [x0, y0], do not precisely correspond to the locations of the highest intensity returns because they take into account the total effect of weighting all intensities within the thresholded data set.

Processing the data to estimate the depth variance, yields Figure 14 which shows that only the central cluster of returns has significant linear extent. While this idea is able to estimate points of roughness, it will be necessary to test the algorithms on data that do come from real roughness with some significant extent along bearing lines.

The estimation of the mean strength of returns along a scan line coming from returns that have significant extent is given by the data in Figure 15 where the means strength (mst) is plotted versus the bearing angle. Most of the returns do not exceed the lower threshold, and so the mst is zero. However, those that are associated with a significant return, show the mst to be between 12 and 15 as expected. A lower mst is an indicator that more than one return is being used in the averaging as shown by Figure 16, and that the distribution is not unimodal. The average mst is lower but is still of interest and could be useful.

What the authors contend is that the hull cleaning Robot will eventually need to be given an [x0, y0] coordinate together with a significant width and depth measure and an intensity measure such as the mst, that could be computed automatically scan by scan . Further work to test the concept is needed.
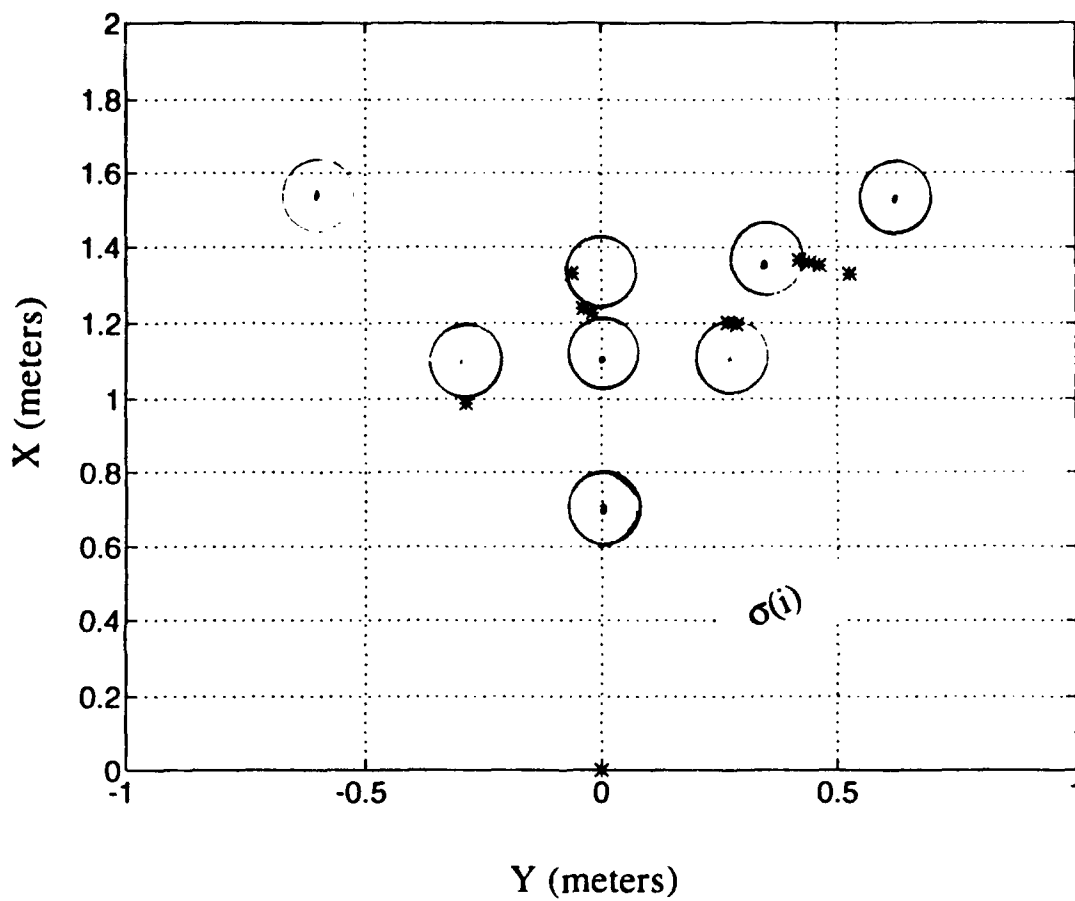
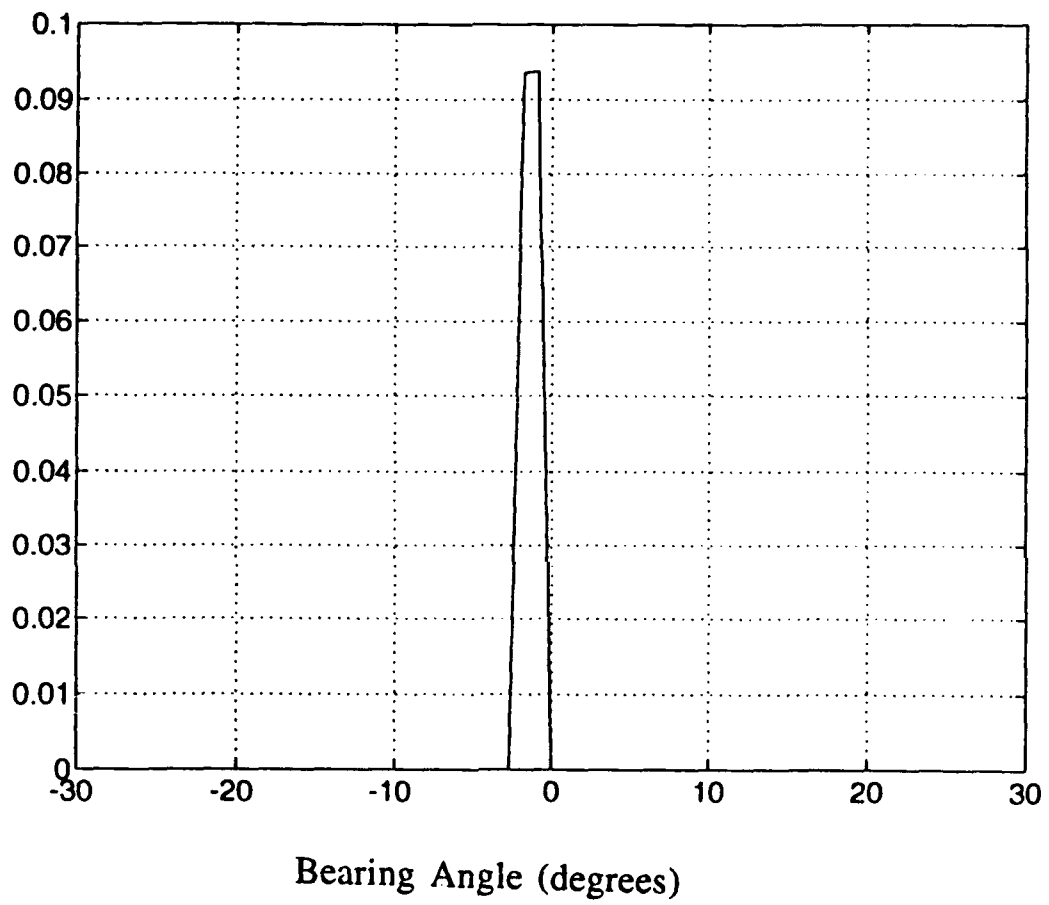Figure 13   X0,Y0 as Computed from Processed Returns
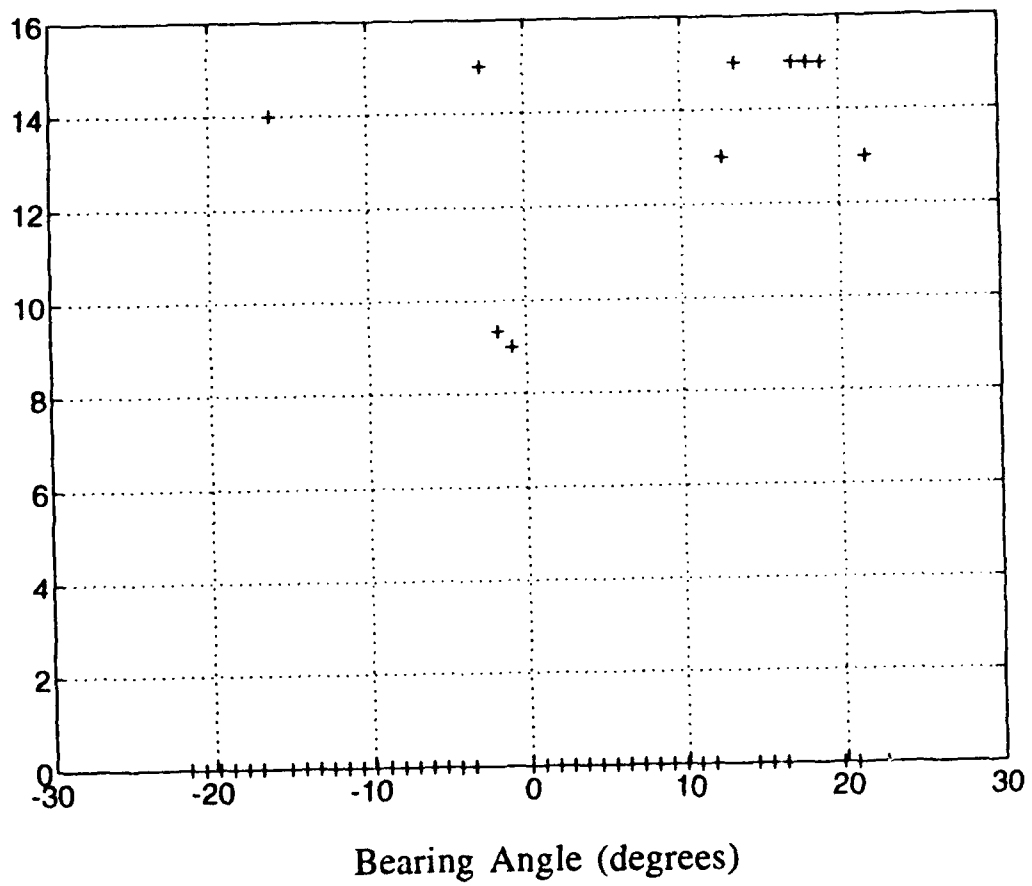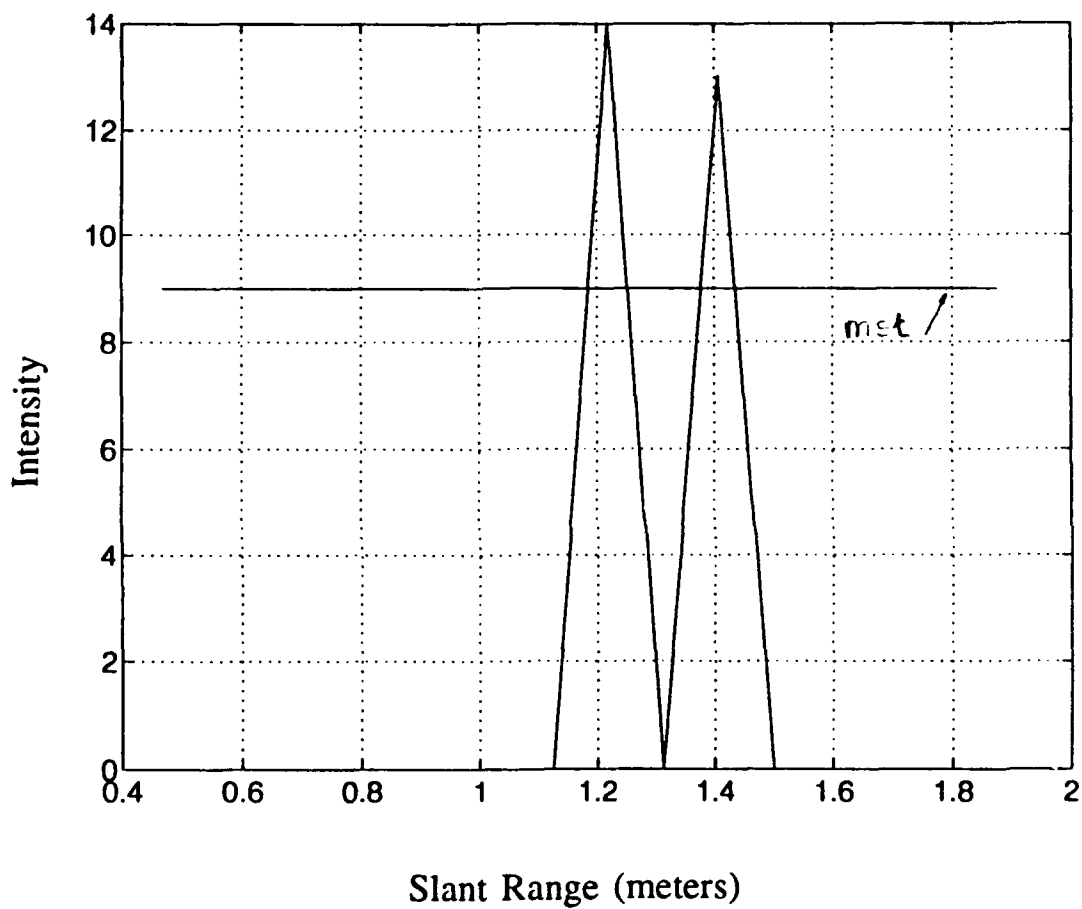
Figure 14 Depth Estimation

Figure 15 Mean Strength Estimation

[Mean Strength as Computed and Intensity versus Slant Range Scanned at Bearing # 24 at -0.9 degrees]

Figure 16 Indication of Multi Modality

CONCLUSION

In conclusion, an initial study has begun to identify whether or not sonar scans of ship plating could be a viable method of determining the location and extend of hull fouling. A simulated set of barnacles using one half inch steel nuts has been ensonified and processing of returns from an ST 725 sonar in one configuration has shown that the locations of significant roughness could indeed be found. What is more, the algorithms presented are expected to lead to a real time capability for an autonomous robot to locate and analyze the sections of hull fouling. A necessary extension of this work is to investigate the ability of the sonar and methods presented here to be successful against real marine growth.

DISTRIBUTION LIST

1. Defense Technical Information Center   2
   Cameron Station
   Alexandria, VA 22314

2. Library   2
   Code 52
   Naval Postgraduate School
   Monterey, CA 93943

3. Professor A.J. Healey   3
   Code ME/Hy
   Naval Postgraduate School
   Monterey, CA 93943

4. Naval Surface Warfare Center   1
   Annapolis, MD 21402-5067